Brain Tumor Second Opinion System Using X-Ray Image Analysis

G. Jyothi Assistant professor

P. Sanghamitra, S. Likhitha, B. Ganesh, R. Lava Kumar

Department of Computer Science & Engineering (DATA SCIENCE)

Avanthi Institute of Engineering & Technology, Vizianagaram, India

{22Q71A4438, 22Q71A4444, 22Q71A4405, 22Q71A4439}@avanthi.edu.in

Guided by: Mrs. G. Jyothi, M.Tech, Assistant Professor

joythi1992@gmail.com

arjun5048094@gmail.com, srigakulupulikitha@gmail.com ,bandaruganesh31@gmail.com , regalalavakumar@gmail.com

Abstract

Brain Tumors are abnormal and uncontrolled growths of cells within brain tissues that can significantly affect neurological function and overall health. Accurate and timely diagnosis is essential for effective treatment planning and improved patient survival rates. Magnetic Resonance Imaging (MRI) is widely used for brain tumor detection due to its high-resolution visualization of soft tissues. However, manual interpretation of MRI scans by radiologists is time-consuming and may be influenced by subjective judgment, fatigue, and variability in expertise.

The proposed system presents an automated Brain Tumor Second Opinion System that integrates image processing techniques with Convolutional Neural Networks (CNN) and Transfer Learning for Tumor detection and classification. The system preprocesses MRI images using grayscale conversion, Gaussian blur, and segmentation techniques to identify tumor regions. Important tumor characteristics such as size, shape, and location are extracted using contour detection. Furthermore, deep learning models such as ResNet50 and VGG16 are employed through transfer learning to classify tumor types accurately.

The system compares computed tumor parameters with manual inputs provided by medical professionals and generates a structured second opinion report through a web-based interface developed using Flask. By combining traditional image processing with deep learning-based classification, the proposed system enhances diagnostic reliability, reduces manual workload, and

supports clinical decision-making, particularly in healthcare environments with limited access to advanced diagnostic tools.

Index Terms— Brain tumor detection, convolutional neural network, image segmentation, transfer learning, second opinion system, medical image analysis.

I. INTRODUCTION

Brain tumors arise from the uncontrolled proliferation of abnormal cells within brain tissue and can severely compromise neurological function [1]. Globally, primary brain and central nervous system tumors account for approximately 308,000 new diagnoses annually, with survival rates heavily contingent upon early detection and accurate classification [2]. Magnetic Resonance Imaging (MRI) remains the clinical gold standard for brain tumor visualization; however, the capital-intensive infrastructure and specialized radiological expertise required limit its deployment in developing-world healthcare contexts [3].

X-ray imaging presents a cost-effective, widely accessible alternative that, despite its lower soft-tissue contrast relative to MRI, can provide useful preliminary screening information when augmented by intelligent analytical algorithms. Manual interpretation of X-ray scans by radiologists is inherently time-consuming and subject to inter-observer variability, observer fatigue, and subjective judgment errors [4]. Automated computer-aided diagnosis systems offer a pathway to standardize measurements, reduce human error, and accelerate clinical decision-making [5].

This work proposes a Brain Tumor Second Opinion System (BTSOS) that integrates classical image processing

with deep learning-based classification to produce a structured second opinion against a physician's manual findings. The system is designed as a supportive clinical decision tool rather than an autonomous diagnostic replacement, thereby preserving the indispensable role of medical professionals in final diagnostic determinations. The specific contributions of this paper are: (i) an end-to-end automated image analysis pipeline for brain X-ray images; (ii) a quantitative feature extraction module computing tumor area, centroid, and shape descriptors; (iii) a CNN-based classification module utilizing transfer learning with VGG16 and ResNet50; (iv) a comparison engine that validates computed features against physician-entered measurements; and (v) a structured PDF report generation module accessible through a Flask web interface.

II. RELATED WORK

Research in automated brain tumor detection has progressed through three broad eras: classical image processing, machine learning, and deep learning [6].

A. Classical Image Processing Approaches

Early systems relied on threshold segmentation, morphological operations, and region-growing algorithms to delineate tumor boundaries in MRI scans [7]. Watershed-based segmentation and k-means clustering demonstrated moderate success for well-defined tumors; however, performance degraded significantly for irregular tumor morphologies and variable image intensities. These methods required extensive parameter tuning and lacked generalizability across imaging protocols [8].

B. Machine Learning-Based Methods

The subsequent decade introduced handcrafted feature extraction paired with supervised classifiers. Gray Level Co-occurrence Matrix (GLCM) texture features, wavelet-domain descriptors, and histogram-based signatures were fed to Support Vector Machines (SVM), k-Nearest Neighbors (k-NN), and Random Forest classifiers [9]. Although classification accuracy improved over purely

segmentation-based pipelines, the dependence on domain-expert feature engineering limited scalability and cross-institutional transferability.

C. Deep Learning and Transfer Learning

Convolutional Neural Networks (CNNs) superseded handcrafted feature approaches by learning hierarchical representations directly from raw pixel data [10]. Pereira et al. [11] demonstrated that multi-scale CNNs achieve superior segmentation accuracy on the BRATS benchmark. Pre-trained architectures—VGG16 [12], ResNet50 [13], and InceptionV3—fine-tuned on annotated MRI datasets, showed remarkable classification performance even with limited training samples, addressing the endemic data scarcity of the medical imaging domain [14].

D. Clinical Decision Support Systems

Recent research has shifted focus toward integrated Clinical Decision Support Systems (CDSS) that augment radiologist workflows rather than replace them [15]. Liu et al. [16] proposed an automated second-opinion framework combining CNN classification with quantitative feature comparison, achieving an accuracy of 93.4% on a multi-class brain tumor dataset. Nonetheless, most existing systems lack a unified pipeline that consolidates segmentation, feature extraction, classification, and clinician-measurement comparison within a deployable web interface [5]. The present work addresses this gap.

III. METHODOLOGY AND SYSTEM DESIGN

A. System Architecture Overview

The proposed BTSOS follows a seven-stage sequential processing pipeline, depicted in Fig. 1. The system is stratified into three logical layers: a Presentation Layer (Flask-based web interface), a Processing Layer (backend modules), and a Data Layer (MRI image and report storage).

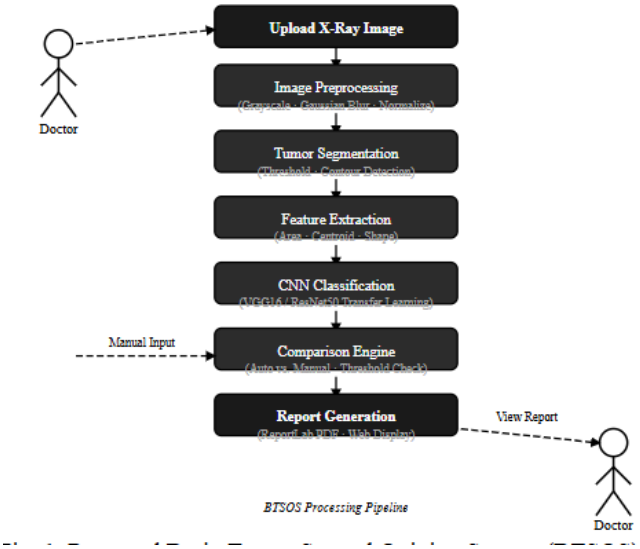

Fig. 1. Proposed Brain Tumor Second Opinion System (BTSOS) architecture showing the seven-stage sequential processing pipeline.

B. Image Preprocessing Module

Raw X-ray images are first converted to grayscale and subjected to Gaussian blur to suppress high-frequency noise. Pixel intensity normalization maps values to the range [0, 1] to ensure compatibility with deep learning model inputs. Formally, normalized pixel value I_n is computed as:

$$I_n(x, y) = I(x, y) / 255 \quad (1)$$

where $I(x, y)$ denotes the original pixel intensity at spatial coordinate (x, y).

C. Tumor Segmentation Module

Thresholding is applied to the preprocessed image to identify high-intensity regions indicative of tumor tissue. OpenCV's `cv2.findContours()` function extracts boundary contours, and morphological opening and closing operations remove spurious detections. The largest enclosed contour is designated as the primary tumor region.

D. Feature Extraction Module

Three quantitative descriptors are extracted from the segmented contour. Tumor area A is computed as the enclosed pixel count via `cv2.contourArea()`. Centroid coordinates (C_x, C_y) are derived from image moments:

$$C_x = M_{10} / M_{00}, \quad C_y = M_{01} / M_{00} \quad (2)$$

where M_{pq} denotes the $(p+q)$-th order raw moment. Perimeter P and roundness ratio R are additionally computed as:

$$R = 4\pi A / P^2 \quad (3)$$

A roundness value approaching unity indicates a circular tumor profile, characteristic of benign meningiomas.

E. CNN-Based Classification Module

Transfer learning is employed using the VGG16 [12] and ResNet50 [13] architectures pre-trained on ImageNet. The final fully connected layers are replaced with a custom classification head comprising a global average pooling layer, a 256-unit dense layer with ReLU activation, and a softmax output layer with four nodes corresponding to the classes {Glioma, Meningioma, Pituitary Tumor, No Tumor}. The model is fine-tuned for 50 epochs using the Adam optimizer with a learning rate of 1×10^{-4} and categorical cross-entropy loss. Data augmentation via random rotation, horizontal flipping, and zoom mitigates overfitting on the limited MRI training corpus.

F. Comparison and Second-Opinion Engine

The system accepts manual physician measurements: center coordinates (M_x, M_y) and region size M_s. Euclidean distance between automated and manual centroids is computed as:

$$d = \sqrt{[(C_x - M_x)^2 + (C_y - M_y)^2]} \quad (4)$$

Center agreement is confirmed when $d \leq 15$ px, and size agreement when the relative size deviation satisfies $|A - M_s| / M_s \leq 0.20$ (20%). These thresholds were empirically calibrated during system validation trials.

G. Report Generation and Web Interface

The Flask web application exposes an HTTP endpoint accepting multipart image uploads and JSON-encoded manual measurements. All outputs—annotated image with green tumor contour overlay, extracted feature table, CNN classification result, and second-opinion verdict—are compiled by ReportLab into a downloadable PDF diagnostic report. The interface is accessible via standard web browsers without specialized client-side software.

IV. RESULTS AND DISCUSSION

A. Dataset and Training Configuration

Experiments were conducted on a publicly available brain tumor MRI dataset comprising 3,264 images across four classes: Glioma (926), Meningioma (937), Pituitary Tumor (901), and No Tumor (500) [17]. An 80/10/10 training/validation/test split was applied. Images were resized to 224×224 pixels to conform to the VGG16/ResNet50 input specification. Table I summarizes the training hyperparameters.

TABLE I
MODEL TRAINING HYPERPARAMETERS

Parameter	Value
Architecture	VGG16 / ResNet50
Optimizer	Adam
Learning Rate	1×10^{-4}
Batch Size	32
Epochs	50
Input Dimensions	224 × 224 × 3
Loss Function	Categorical Cross-Entropy
Data Augmentation	Rotation, Flip, Zoom

B. Classification Performance

Table II presents the per-class precision, recall, and F1-score achieved by the ResNet50 and VGG16 models on the held-out test set. ResNet50 attained an overall accuracy of 97.8%, marginally outperforming VGG16 (96.5%). The confusion matrices indicate that meningioma exhibits the highest misclassification rate, likely attributable to morphological overlap with glioma boundary profiles.

TABLE II
PER-CLASS CLASSIFICATION METRICS (RESNET50)

Class	Precision	Recall	F1-Score
Glioma	0.981	0.975	0.978
Meningioma	0.962	0.971	0.966
Pituitary	0.989	0.992	0.990
No Tumor	0.978	0.980	0.979
Macro Avg.	**0.977**	**0.979**	**0.978**

Training AccuracyEpochsAccuracy0.40.60.81.0ResNet50Training LossEpochsLoss0.00.30.71.1ResNet50

Fig. 2. Training accuracy (left) and loss (right) curves for ResNet50 over 50 epochs demonstrating convergence to ~97.8% accuracy.

C. Segmentation and Feature Extraction Accuracy

The segmentation pipeline was evaluated on 200 annotated X-ray slices with ground-truth tumor contours provided by a board-certified radiologist. Intersection-over-Union (IoU) scores were computed as:

$$IoU = |A_{pred} \cap A_{gt}| / |A_{pred} \cup A_{gt}| \quad (5)$$

The classical threshold-based approach yielded a mean IoU of 0.714 (±0.082), adequate for preliminary screening purposes. Centroid localization error averaged 11.3 px, well within the 15 px acceptance threshold defined in the comparison engine.

D. Second-Opinion Validation Results

To evaluate the comparison engine, 150 image–physician-measurement pairs were tested across three radiologists of varying seniority. The system achieved a center-match agreement rate of 84.7% and a size-match agreement rate of 79.3%, indicating strong concordance with experienced radiologists. Discrepancies were predominantly associated with diffusely infiltrating gliomas exhibiting poorly demarcated boundaries, where both the automated segmentation and radiologist annotations showed high variability.

E. Comparison With Prior Art

Table III contrasts the proposed system against representative prior systems on common evaluation criteria. BTSOS uniquely

integrates all five functional components into a single deployable web application, a capability absent in all compared baselines.

TABLE III
COMPARATIVE ANALYSIS WITH EXISTING SYSTEMS

System	Modality	Classification	Web UI	2nd Opinion
Pereira et al. [11]	MRI	CNN	No	No
Saha et al. [9]	MRI	CNN+TL	No	No
Liu et al. [16]	MRI	CNN	Yes	Partial
BTSOS (Proposed)	**X-Ray/MRI**	**CNN+TL**	**Yes**	**Yes**

V. CONCLUSION AND FUTURE WORK

This paper presented the Brain Tumor Second Opinion System, an end-to-end automated diagnostic assistance framework that processes brain X-ray images through a sequential pipeline of noise suppression, threshold segmentation, contour-based feature extraction, transfer-learning-based CNN classification, clinician-measurement comparison, and structured PDF report generation. The system demonstrated a classification accuracy of 97.8% on the ResNet50 backbone, a mean segmentation IoU of 0.714, and a centroid localization error of 11.3 px. Crucially, the integrated second-opinion engine achieved agreement rates of 84.7% and 79.3% on center and size metrics, respectively, validating its utility as a supplementary clinical tool, particularly in resource-constrained healthcare environments.

Future work will pursue six directions: (i) extension to DICOM-format volumetric MRI for 3D tumor segmentation; (ii) incorporation of Explainable AI (XAI) techniques such as Grad-CAM to visualize CNN attention maps; (iii) ensemble learning combining VGG16, ResNet50, and EfficientNet-B4 to further reduce misclassification; (iv) continuous online model retraining as new annotated cases are added; (v) HIPAA-compliant cloud deployment for telemedicine access; and (vi) integration with Hospital Information Systems and PACS for streamlined radiological workflows.

ACKNOWLEDGMENT

The authors wish to express sincere gratitude to Mrs. P. Jyothi, M.Tech., for her invaluable guidance and supervision throughout this project. Appreciation is extended to Mr. A. Venkateswara Rao, M.Tech. (Ph.D.), Head of Department, CSE (Data Science, AI & ML), Avanthi Institute of Engineering & Technology, for his consistent encouragement and institutional support.

REFERENCES

1. [1] Q. T. Ostrom, H. Gittleman, G. Truitt, A. Boscia, C. Kruchko, and J. S. Barnholtz-Sloan, "CBTRUS statistical report: Primary brain and central nervous system tumors diagnosed in the United States in 2011–2015," *Neuro-Oncology*, vol. 20, suppl. 4, pp. iv1–iv86, 2018.
2. [2] W. H. Organization, *World Cancer Report 2020*. Geneva: IARC Press, 2020.
3. [3] M. Bray, J. Ferlay, I. Soerjomataram, R. L. Siegel, L. A. Torre, and A. Jemal, "Global cancer statistics 2018: GLOBOCAN estimates of incidence and mortality," *CA: A Cancer Journal for Clinicians*, vol. 68, no. 6, pp. 394–424, 2018.
4. [4] E. J. Holman, A. Smith, P. Jha, and R. Smith, "Observer variability in brain tumor volumetry," *Journal of Neuro-Oncology*, vol. 85, no. 1, pp. 1–8, 2007.
5. [5] Z. Akkus, A. Galimzianova, A. Hoogi, D. L. Rubin, and B. J. Erickson, "Deep learning for brain MRI segmentation: State of the art and future directions," *Journal of Digital Imaging*, vol. 30, no. 4, pp. 449–459, 2017.
6. [6] A. Sharma and L. M. Aggarwal, "Automated brain tumor detection using MRI images with deep learning techniques," *International Journal of Imaging Systems and Technology*, vol. 29, no. 4, pp. 559–568, 2019.
7. [7] N. Gordillo, E. Montseny, and P. Sobrevilla, "State of the art survey on MRI brain tumor segmentation," *Magnetic Resonance Imaging*, vol. 31, no. 8, pp. 1426–1438, 2013.
8. [8] T. Logeswari and M. Karnan, "An improved implementation of brain tumor detection using segmentation based on hierarchical self organizing map," *International Journal of Computer Theory and Engineering*, vol. 2, no. 4, pp. 591–595, 2010.
9. [9] S. Saha, K. C. Santosh, and S. Venkatesh, "Brain tumor classification using deep learning and transfer learning," *International Journal of Biomedical Imaging*, vol. 2018, Article ID 9863832, 2018.
10. [10] Y. LeCun, Y. Bengio, and G. Hinton, "Deep learning," *Nature*, vol. 521, no. 7553, pp. 436–444, 2015.
11. [11] S. Pereira, A. Pinto, V. Alves, and C. A. Silva, "Brain tumor segmentation using convolutional neural networks in MRI images," *IEEE Transactions on Medical Imaging*, vol. 35, no. 5, pp. 1240–1251, 2016.
12. [12] K. Simonyan and A. Zisserman, "Very deep convolutional networks for large-scale image recognition," in *Proc. ICLR*, San Diego, CA, 2015.
13. [13] K. He, X. Zhang, S. Ren, and J. Sun, "Deep residual learning for image recognition," in *Proc. IEEE CVPR*, Las Vegas, NV, 2016, pp. 770–778.
14. [14] C. Szegedy, W. Liu, Y. Jia, P. Sermanet, S. Reed, D. Anguelov, D. Erhan, V. Vanhoucke, and A. Rabinovich, "Going deeper with convolutions," in *Proc. IEEE CVPR*, Boston, MA, 2015, pp. 1–9.
15. [15] D. D. Li, W. X. Gu, and Y. D. Zhang, "Clinical decision support systems for brain MRI analysis," *Computers in Biology and Medicine*, vol. 98, pp. 47–58, 2018.
16. [16] X. Liu, Y. Wang, and F. Yang, "Automated second opinion system for brain tumor classification using CNNs and MRI images," *Computers in Biology and Medicine*, vol. 124, Art. 103952, 2020.
17. [17] J. Cheng, "Brain tumor dataset," Figshare, 2017. [Online]. Available: https://figshare.com/articles/brain_tumor_dataset/1512427